Eur Biophys J (2010) 39:1167–1176
DOI 10.1007/s00249-009-0569-z

ORIGINAL PAPER

Investigation of stratum corneum lipid model membranes with free fatty acid composition by neutron diffraction

Natalia Yu. Ryabova · M. A. Kiselev · S. Dante · T. Hauß · A. M. Balagurov

Received: 14 September 2009 / Revised: 20 November 2009 / Accepted: 24 November 2009 / Published online: 15 December 2009

Abstract The outermost epidermal layer, the stratum corneum (SC), is the main skin barrier. Studies of SC model systems enable characterization of the influence of individual lipids on the organization of the SC lipid matrix, which is the main pathway of water through the skin. This work presents a neutron diffraction study of the SC model membranes based on short-chain ceramide 6 with nearly realistic composition of free fatty acids (FFA) at physiological temperature of the SC. The influence of FFA and the effect of cholesterol–cholesterol sulfate substitution on the structure and hydration of the SC model membranes are described. The structure of the SC membrane with FFA is close to the structure of the earlier studied SC membrane based on short-chain palmitic acid (PA) and does not vary significantly under changes of the ratio of the main membrane components. FFA accelerates membrane swelling at the same low level of hydration of both PA- and FFA-containing membranes. The substitution of cholesterol sulfate by cholesterol in the membrane composition decreases membrane swelling and leads to phase separation in the model system.

Keywords Neutron diffraction · Stratum corneum · Model lipid membrane · Hydration

Abbreviations

CER6	*N*-(α-hydroxyoctadecanoyl)-phytosphingosine
PA	Palmitic acid
Ch	Cholesterol
ChS	Cholesterol sulfate

Introduction

The outer protective layer of mammalian skin, the stratum corneum (SC), plays a key role as a barrier to penetration of molecules through the skin and prevents water loss. SC structure can be roughly described by the "bricks and mortar" model, in which horny cells (corneocytes) are embedded in a lamellar lipid matrix. The corneocytes correspond to the bricks while the lipids fill the intercellular space like mortar. The major components of the SC lipid matrix are: ceramides, fatty acids, cholesterol, and cholesterol esters (Lampe et al. 1983; Robson et al. 1994). Ceramides account for approximately 50% of the total SC lipid mass. Human SC includes nine structurally heterogeneous types of ceramide, termed CER1 to CER9. Cholesterol represents about 25% of the lipids, and free fatty acids amount to about 10% of the lipid mass. The most abundant free fatty acids are saturated long-chain C22 and C24 acids. There are small proportions of cholesterol derivatives, but phospholipids are absent.

N. Yu. Ryabova (✉) · M. A. Kiselev · A. M. Balagurov
Frank Laboratory of Neutron Physics,
Joint Institute for Nuclear Research,
141980 Dubna, Moscow Region, Russia
e-mail: rny03@nf.jinr.ru

N. Yu. Ryabova
Skobeltsyn Institute of Nuclear Physics,
Moscow State University, Moscow, Russia

S. Dante · T. Hauß
Helmholtz-Zentrum Berlin für Materialien und Energie,
Berlin, Germany

T. Hauß
Institute of Biochemistry, Physical Biochemistry,
Technische Universität Darmstadt, Darmstadt, Germany

In accordance with modern thinking, the SC lipid matrix is the main pathway for water diffusion through the skin. In this way, the SC barrier is determined by the nature of the intercellular lipids. For this reason many investigations of SC organization have been performed over the last 40 years with the purpose of determining the role of each type of lipid in the formation of the SC lipid matrix and its properties. Freeze-fracture electron microscopy shows that the intercellular lipids are organized in lamellae sheets with periodicity of approximately 110–140 Å (Breathnach et al. 1973). The repeating unit of about 130 Å consisting of a broad-narrow-broad sequence was first detected in the lamellar organization of mouse SC by electron microscopy (Madison et al. 1987). Further X-ray diffraction investigations of mammalian SC revealed the presence of two lamellar phases with periodicities of approximately 64 Å (short-periodicity phase) and 130 Å (long-periodicity phase) (White et al. 1988; Bouwstra et al. 1991). The long-periodicity phase was also observed in lipid suspension containing a mixture of the main SC lipid components and depended on the presence of particular ceramides (McIntosh et al. 1996). Bouwstra and co-workers proposed the so-called sandwich model of the SC matrix, where the long-chain CER1 and CER4 molecules play a crucial role in the formation of the long-periodicity phase (Bouwstra et al. 2000). However, an increase in water content in native SC leads to the disappearance of the 130-Å lamellar phase. This 130 Å lamellar repeat distance was not confirmed in other X-ray diffraction studies (Garson et al. 1991) or neutron diffraction studies of hydrated porcine SC (Charalambopoulou et al. 2002). The long-periodicity phase of 130 Å was not observed in neutron diffraction experiments with the SC model lipid membrane with long-chain ceramide either (Kessner et al. 2008).

In comparison with the viable epidermis, a low degree of hydration is a characteristic feature of SC. It is well known that SC intercellular lipids play an essential role in water-holding capacity and prevention of transepidermal water loss (Elias 1983). Although the exact mechanism of SC swelling is not clear, the general description of it was given in previous studies. Small-angle neutron scattering (SANS) investigation of porcine SC, at water content below 16%, reveals that water is absorbed by the intercellular region and that water uptake is very small. At relative humidity between 16% and 84%, water is also absorbed by corneocytes. As relative humidity increases to full hydration, most water is taken up by corneocytes (Charalambopoulou et al. 1998). Norlen and coworkers proposed that, in fully hydrated SC, the intercellular lipids prevent attraction between the adjacent corneocytes and thereby control the swelling of the whole system (Norlén et al. 1997).

Previous investigations have shown that both neutron and X-ray diffraction are the most powerful techniques for analysis of model systems simulating native SC lipids isolated from native SC (Bouwstra et al. 1996) and synthetic lipid mixtures (McIntosh 2003; Jager et al. 2004). Diffraction methods allow the characterization of the internal membrane structure via analysis of the scattering length density distribution across the bilayer calculated from the Fourier transform of the diffraction pattern. However, model membrane with complexes of ceramides is often an inhomogeneous system and therefore is inappropriate for characterization by this method. Diffraction patterns from native SC often do not contain enough Bragg reflections for analysis of the scattering length density distribution recovered from it (Charalambopoulou et al. 2002). Application of neutron diffraction with Fourier profile analysis is a very effective technique for investigation of model SC lipid membranes with individual ceramides. In particular, it has been established that a model SC lipid membrane based on CER6 and palmitic acid is characterized by a low level of hydration of the interbilayer space and considerably slower process of water diffusion through it in comparison with phospholipid membranes (Kiselev et al. 2005). To explain these membrane features, a hypothesis of armature reinforcement of the lipid matrix due to the fully extended (FE) conformation of ceramide 6 molecules pulling together neighboring bilayers has been suggested (Kiselev 2007). Recently the influence of the chain length of free fatty acids on CER6-based SC model membranes has been examined (Ruettinger et al. 2008). An increase in the chain length of the fatty acids does not lead to alteration of the internal nanostructure but decreases the membrane repeat distance from 45.6 Å (palmitic acid, C16:0) to 43.7 Å (cerotic acid, C26:0) due to partial interdigitation of the fatty acid chains. Free fatty acids with longer chains tend to form a separate so-called fatty-acid-rich phase. Using small-angle X-ray diffraction on multilamellar vesicle and SANS on unilamellar vesicle, the influence of cholesterol on the model membrane consisting of four SC lipids at different states has been investigated (Zbytovska et al. 2008). An increase in cholesterol concentration in the membrane causes a decrease in the order of the hydrocarbon chains and enhances the fluidity of the SC lipid membranes at 32°C. In spite of its low concentration (about 2% w/w of the SC lipids), cholesterol sulfate (ChS) plays a significant role in several skin processes such as keratinocyte differentiation, desquamation, and cholesterol metabolism (Elias et al. 2008; Strott and Higashi 2003). Furthermore, intercellular cohesion in SC is associated with the presence of ChS. A reduction in ChS content decreases the stabilization of the lamellar phase in deep layers of the SC. The presence of ChS promotes the solubility of cholesterol and thereby reduces the formation of cholesterol crystalline domains in SC model mixtures (Bouwstra et al. 1999). It is significant

that the influence of ChS on SC lipid organization and its barrier properties often depends on Ch levels. For example, in diseased skin of patients with recessive X-linked ichthyosis, abnormalities in cholesterol–cholesterol sulfate ratio in the lipid composition are observed (Williams and Elias 1981). Both a tenfold increase in ChS content and a 50% reduction in Ch are assumed to be responsible for abnormal barrier function in recessive X-linked ichthyosis (Zettersten et al. 1998). Although there are several studies focusing on the role of ChS in SC, little is known about its influence on hydration of SC.

This work is part of a systematical study of SC model membranes with individual short-chain ceramides by means of neutron diffraction. In our previous studies CER6 was chosen among six types of short-chain ceramides present in human SC (Kiselev et al. 2005). In the work described herein we studied the influence of a realistic mixture of free fatty acids (FFA) on the structure and hydration of SC model membranes. We used a mixture of different free fatty acids similar to that in the native SC composition, which includes palmitic acid, stearic acid, arachidic acid, behenic acid, lignoceric acid, and cerotic acid in molar ratio of 1.3/3.3/6.8/42.0/36.2/6.7 (Bouwstra et al. 1998). Although CER6 is a minor component of SC ceramides, we proceeded to use it to compare the systems based on FFA with membranes comprising only palmitic acid. To characterize the effect of cholesterol–cholesterol sulfate substitution on hydration of SC model membranes with CER6, we studied the kinetics of swelling of two samples with different cholesterol–cholesterol sulfate ratios.

Materials and methods

Sample preparation

N-(α-hydroxyoctadecanoyl)-phytosphingosine (CER6) was a gift from Cosmoferm (Delft, The Netherlands). Cholesterol (Ch), cholesterol sulfate (ChS), palmitic acid (PA), stearic acid (SA), arachidic acid (AA), behenic acid (BA), lignoceric acid (LA), and cerotic acid (CA) were purchased from Sigma–Aldrich (Russia). Quartz plates were purchased from Spectrosil 2000, Saint-Gobain (Germany).

The quaternary system CER6/Ch/FFA/ChS with three different component ratios (55/20/15/10, 66/10/18/6, and 60/20/15/5) was prepared. The proportions of lipid components were chosen to be the same as in previously investigated membranes with only palmitic acid (Kiselev et al. 2005).

To obtain the free fatty acid composition, palmitic acid (C16:0), stearic acid (C18:0), arachidic acid (C20:0), behenic acid (C22:0), lignoceric acid (C24:0), and cerotic acid (C26:0) were mixed in molar ratio of 1.3/3.3/6.7/41.7/36/6.7. The chemical structure of the free fatty acid molecules with the shortest (palmitic acid) and longest carbon chains (cerotic acid), ceramide 6, cholesterol, and cholesterol sulfate molecules are shown in Fig. 1. Appropriate mixtures of lipids were dissolved in chloroform/methanol (2/1 w/w) at concentration of 10 mg/ml. To prepare the samples, 3 g of solution was spread over a 6.4 cm × 2.5 cm quartz plate. The thickness of the lipid film on the quartz slide was $t = 18.8$ μm. To prepare a sample for the kinetic experiment, 1.8 g of solution was spread over a 6.4 cm × 1.4 cm quartz plate.

The samples were dried on a warm plate (≈40°C) and were then placed in a vacuum desiccator to remove remaining solvent. Samples were heated in horizontal orientation at 80°C during 30 min. This annealing step was applied to decrease the mosaicity of the samples and thereby improve their scattering ability. After annealing, samples were gradually cooled to room temperature and hydrated for 3 h with water vapor at 100% relative humidity.

Neutron diffraction experiments

Neutron diffraction experiments on the oriented sample were carried out on the V1 membrane diffractometer at the Berlin Neutron Scattering Centre of the Helmholtz Center

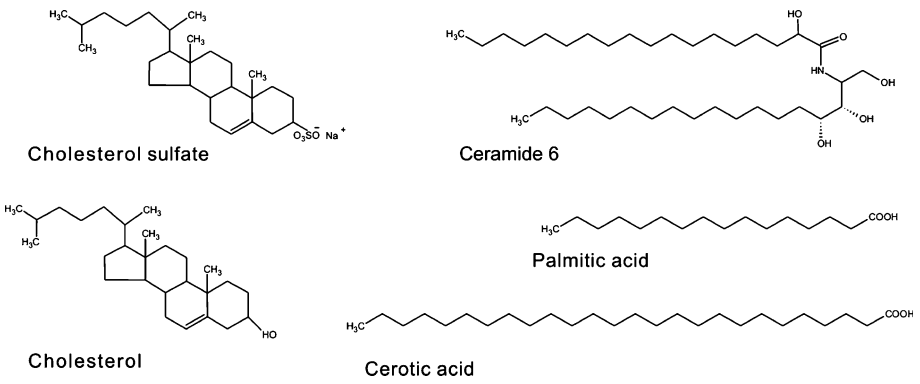

Fig. 1 Chemical structure of ceramide 6, cholesterol, cholesterol sulfate, and the fatty acid (palmitic and cerotic) molecules

Berlin for Materials and Energy (Berlin, Germany). A diffraction pattern was obtained by rocking the sample at different fixed angles of the two-dimensional position-sensitive ^{3}He detector (20 × 20 cm^2 area, 1.5 × 1.5 mm^2 spatial resolution). The neutron wavelength λ and sample-to-detector distance were 5.23 Å and 102.38 cm, respectively.

Multilamellar membranes CER6/Ch/FFA/ChS with component mass ratio of 55/20/15/10, 66/10/18/6, and 60/20/15/5 were characterized by neutron diffraction at 57% relative humidity (RH), which was maintained by saturated NaBr salt solution. Before each measurement, samples were equilibrated for 24 h in a chamber with water vapor at fixed temperature.

Data analysis

Neutron diffraction gives insight into the internal nanostructure via analysis of the scattering length density distribution $\rho(z)$ across the bilayer, calculated by Fourier transform of the diffraction pattern (Worcester and Franks 1976; Schoenborn 1976; Bueldt et al. 1978). In case of lamellar diffraction, when the structure factors are measured only along the direction perpendicular to the membrane surface, one can obtain a projection of the scattering length density distribution onto this direction (normally termed the Fourier profile):

$$\rho(z) = \iint \rho(x,y,z)\mathrm{d}x\mathrm{d}y = a + b\sum_{h=1}^{h_{\max}} F_h \cos\left(\frac{2\pi hz}{d}\right). \quad (1)$$

The absolute values of the structure factors $|F_h| = (I_h/LA_h)^{1/2}$ were calculated from the scattering intensity of the diffraction peak I_h and corrected for the Lorentz factor $L = 1/\sin 2\theta_h$ for rotating oriented membrane in case of a monochromatic neutron beam. Here h is the order of diffraction peak. The absorption correction was taken into account as the absorption coefficient A_h:

$$A_h = \frac{\sin\theta_h}{2\mu t}\cdot\left[1 - \exp\left(-\frac{2\mu t}{\sin\theta_h}\right)\right].$$

Here μ is the linear absorption coefficient and t is the thickness of a sample. The absorption coefficient of matter is calculated as $\rho\frac{N_A}{M}(\sigma_{abs} + \sigma_{scatt})$, where N_A is the Avogadro constant, M is the molecular weight, ρ is the specific density, σ_{abs} is the total cross-section, and σ_{scatt} is the scattering cross-section. For multilamellar lipid membranes the linear absorption coefficient depends on the kind of lipids, the thickness of the lipid bilayer, the value of the interbilayer space, and the molar ratio of D_2O in the water in this space. Using the values of lipids and water linear absorption coefficients, one can calculate the product μt. This parameter has similar values of 0.0111 and 0.0113 for 55/20/15/10 and 66/10/18/6 membranes at 8% D_2O, respectively.

The phases of the structure factors were determined from H_2O/D_2O exchange experiments. For centrosymmetric structures the structure factors change linearly with the isotopic composition of the water, as described elsewhere (Worcester and Franks 1976; Franks and Lieb 1979). In our case a center of symmetry was chosen to be at the center of the bilayer and the water distribution peaks resembling Gaussian shape are centered at $\pm d/2$ so that, when H_2O is replaced by D_2O, the even-order structure factors must increase but the odd-order structure factors must decrease algebraically. Phases assigned according to this rule for the CER6/Ch/FFA/ChS membranes with both 55/20/15/10 and 66/10/18/6 compositions are: −, +, −, +, and − for the first, second, third, fourth, and fifth diffraction order, respectively.

The coefficients a and b in (1) were determined in the procedure of Fourier profile normalization using values of the neutron scattering length density of methyl group ($SLD_{CH3} = -0.0085 \times 10^{-12}$ cm^{-2}) and methylene group ($SLD_{CH2} = -0.0031 \times 10^{-12}$ cm^{-2}). The neutron scattering length density of molecular group is calculated as: $SLD = \sum_{i=1}^{n} b_c/V_m$, where b_c is the coherent neutron scattering length of the ith of n atoms in a molecular group with molecular volume V_m.

The absolute error of the scattering length density profile was calculated as an error of the indirect measurable parameter from the following equation:

$$\Delta\rho_{exp}(z) = b\left[\sum_{h=1}^{h_{\max}} (\Delta F_h)^2 \cos^2\left(\frac{2\pi hz}{d}\right)\right]^{1/2}. \quad (2)$$

The errors of the structure factors ΔF_h were calculated taking into account the statistics of signal (scattering intensity) and background and are given in Table 1.

To characterize the internal membrane structure quantitatively, a simulation of the Fourier profile by a sum of Gaussian functions, which corresponds to the main molecular groups as described by Rand and Luzzati (1968), was used. The region of polar head groups, methylene groups, and cholesterol molecules was fitted by the function

$$\rho^{sym}(z) = \frac{A}{\sqrt{2\pi}\sigma} \cdot \left(\exp\left[-\frac{1}{2}\cdot\left(\frac{z-z_0}{\sigma}\right)^2\right] + \exp\left[-\frac{1}{2}\cdot\left(\frac{z+z_0}{\sigma}\right)^2\right]\right),$$

which describes the symmetrical scattering length density distribution relative to $z = 0$. This function has three fit parameters: the area A, the standard deviation σ, and z_0. To characterize the width and position of a molecular group, $FWHM = 2\sigma\sqrt{2\ln 2}$ and z_0 are used, respectively. The

Table 1 Experimental structure factors of the CER6/Ch/FFA/ChS membranes corrected as described in the text

	F_1 (a.u.)	F_2 (a.u.)	F_3 (a.u.)	F_4 (a.u.)	F_5 (a.u.)
55/20/15/10					
20°C	14.63 ± 0.01	4.66 ± 0.04	5.62 ± 0.03	2.90 ± 0.10	2.94 ± 0.09
32°C	14.50 ± 0.02	4.78 ± 0.07	5.55 ± 0.03	2.86 ± 0.26	3.04 ± 0.28
66/10/18/6					
20°C	16.45 ± 0.01	6.51 ± 0.03	7.10 ± 0.04	3.19 ± 0.06	3.08 ± 0.06
32°C	15.48 ± 0.02	6.04 ± 0.03	6.67 ± 0.09	2.95 ± 0.29	2.88 ± 0.22

function corresponding to the methyl group centered at $z = 0$ is given by the following equation:

$$\rho_{CH_3}(z) = \frac{A}{\sqrt{2\pi}\sigma} \cdot \exp\left[-\frac{1}{2} \cdot \left(\frac{z - z_0}{\sigma}\right)^2\right].$$

Thus, the Fourier profile was simulated by the following function with 11 independent parameters:

$$\rho_{fit}(z) = \rho^{sym}_{PH}(z) + \rho^{sym}_{Chol}(z) + \rho^{sym}_{CH_2}(z) + \rho_{CH_3}(z). \quad (3)$$

Calculation of these parameters was performed by least-squares method using PeakFit software (System Software Inc.).

Water $\rho_w(z)$ across the bilayer was calculated as a difference between Fourier profiles restored at 50% and 8% D_2O content in water vapor.

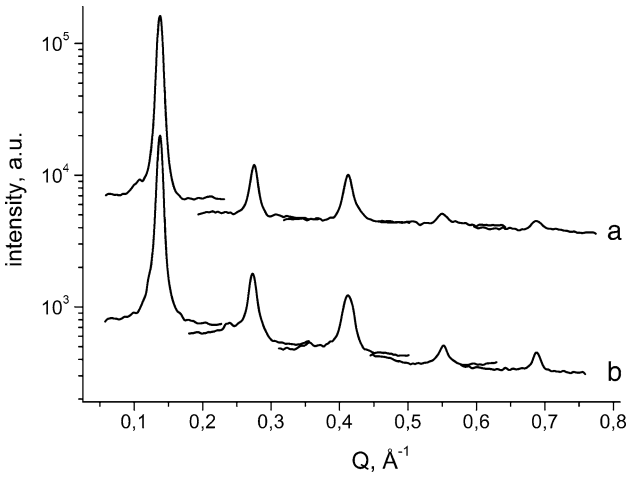

Fig. 2 Rocking curves for the compositions *a* 55/20/15/10 and *b* 66/10/18/6 at five different detector angles at 8% D_2O, 57% RH, at temperature of 20°C

Results

Structure

The samples were measured at the nominal temperatures of 32°C (physiological temperature of SC) and 20°C and 57% RH. As shown below, the composition 55/20/15/10 is less homogeneous at 32°C as compared with at 20°C. The composition 66/10/18/6 is more resistant to changes of experimental conditions in this temperature alteration. Therefore, to obtain the accurate signs of structure factors (see below) we investigated 55/20/15/10 and 66/10/18/6 compositions at various heavy-water concentrations at 20°C and 32°C, respectively. Figure 2 presents the neutron diffraction spectra with five diffraction orders for the membranes with compositions 55/20/15/10 and 66/10/18/6 measured at temperature of 20°C, 57% RH, and 8% D_2O.

The averaged repeat distance of the 55% CER6/20%Ch/15%FFA/10%ChS membrane $d = 45.67 \pm 0.02$ Å was calculated from Bragg peak positions at various H_2O/D_2O contrasts. The higher diffraction orders at temperature of 32°C show that the system is not completely homogeneous and has a minor phase with repeat distance $d^{minor} = 44.0 \pm 0.2$ Å. The membrane repeat distance of the main phase at 32°C is slightly less than that at 20°C: $d = 45.44 \pm 0.06$ Å.

The membrane with the composition 60/20/15/5 at 32°C as well as the composition 55/20/15/10 is a quasihomogeneous system with periodicity of 45.71 ± 0.06 Å and has a minor second phase with periodicity of 44.4 ± 0.4.

The spectra of the 66%CER6/10%Ch/18%FFA/6%ChS membrane are characterized by the evident diffraction peak from the second structure phase present. The averaged repeat distances of this composition at 20°C and 32°C are equal to 45.7 ± 0.2 Å and 45.6 ± 0.2 Å, respectively, and are close to those of the compositions 55/20/15/10 and 60/20/15/5. The repeat distance of minor phase at both temperatures has a value of $d^{minor} = 52.9 \pm 0.1$ Å.

The neutron scattering length density distributions for the CER6/Ch/FFA/ChS membranes calculated and simulated in accordance with Eqs. (1) and (3) are presented in Fig. 3. The confidence limit for the scattering length density profile was estimated according to Eq. (2). The Fourier profiles for the CER6/Ch/FFA/ChS membranes exhibit a very small intermembrane space at 57% RH, which is characteristic for the 55%CER6/25%Ch/15%PA/5%ChS membrane (Kiselev et al. 2005). The difference between the neutron scattering length density profiles for both 55/20/15/10 and 66/10/18/6 compositions at 20°C and 32°C is comparable with the error in these profiles.

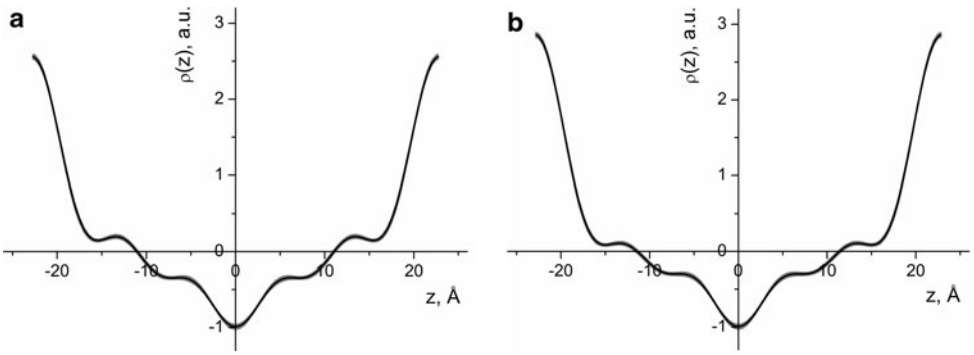

Fig. 3 The neutron scattering length density $\rho(z)$ of the CER6/Ch/FFA/ChS membrane with compositions **a** 55/20/15/10 and **b** 66/10/18/6 at 8% D_2O, 32°C, and 57% RH. The *grey shaded* area indicates the error of the neutron density profile

Despite low hydration of the intermembrane space, the water distribution function $\rho_w(z)$ exhibits penetration of water into the hydrocarbon chains region, similar to the case of SC_PA membrane. As described by Kiselev et al. (2005) the hydrophobic–hydrophilic (HH) boundary is given by the coordinate z_{HH}, determined as the first zero of the water distribution function, where the probability for water molecule location becomes negligibly small. The obtained results are presented in Fig. 4. The HH boundary z_{HH} amounts to 15.0 ± 0.2 and 14.7 ± 0.2 Å for the 55/20/15/10 and 66/10/18/6 compositions, respectively. The main parameters of the SC membranes are summarized in Table 2.

Membrane hydration

To reveal the effect of cholesterol sulfate versus cholesterol on the progress of the SC lipid model membrane hydration, the kinetics of swelling of the CER6/Ch/FFA/ChS membranes with the compositions 55/20/15/10 and 55/30/15/0 was measured by time-resolved diffraction technique at 20°C.

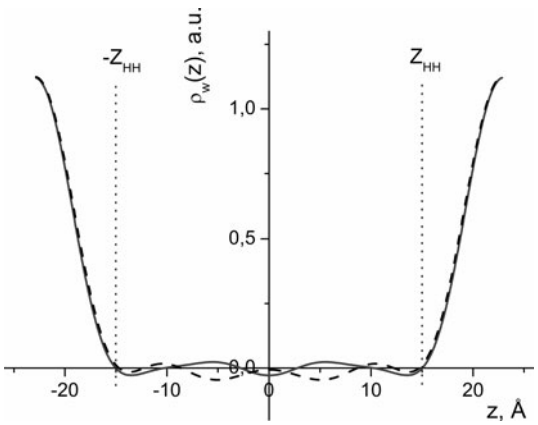

Fig. 4 Water distribution function $\rho_w(z)$ across the CER6/Ch/FFA/ChS membranes with compositions 55/20/15/10 at $T = 20$°C and 59% RH (solid grey line) and 66/10/18/6 at $T = 32$°C and 55% RH (*dashed black line*). The hydrophobic–hydrophilic boundary is indicated by the *dotted line*

55%CER6/20%Ch/15%FFA/10%ChS membrane

A dry sample was introduced into the chamber with excess heavy water, and the first-order diffraction peak from the 55%CER6/20%Ch/15%FFA/10%ChS membrane was collected repeatedly for 7 h with acquisition time of 10 min. For the next 13.4 h four orders were collected one after another with acquisition time of 13, 20, 20, and 32 min, respectively. Figure 5 presents the change in the membrane repeat distance during the hydration process. The membrane swelling is described by the exponential

$$d(t) = d_{fh} - \Delta d \cdot \exp\left(-t/\tau\right) \quad (4)$$

with characteristic time of $\tau = 61 \pm 2$ min. Due to hydration the repeat distance increases by $\Delta d = 1.24 \pm 0.02$ Å from 44.75 ± 0.50 Å in the dry state at room humidity to $d_{fh} = 45.99 \pm 0.01$ Å in the fully hydrated state.

Figure 6 presents the time dependence of the structure factors F_h during the hydration process. At the beginning of hydration for the first 2 h, F_1 increases exponentially with characteristic time of 34 ± 2 min (only the first 11 points were fitted). Then the time dependence $F_1(t)$ becomes constant and, finally, decreases linearly. The structure factors of the higher diffraction orders decrease linearly too.

55%CER6/30%Ch/15%FFA membrane

The first diffraction peak from the 55%CER6/30%Ch/15%FFA membrane was collected for 9.7 h. For the next 8 h four orders were collected. Swelling of this membrane is described by Eq. (4) with characteristic time of 67 ± 4 min and $\Delta d = 0.63 \pm 0.02$ Å (Fig. 5) and completed within about 6 h as well as swelling of the cholesterol sulfate-containing membrane. The time dependence of F_1 has behavior analogous to that of the membrane with ChS. In the absence of ChS, the fully hydrated membrane

Table 2 Structure parameters of the partially hydrated CER6/Ch/FFA/ChS membranes with the compositions 55/20/15/10 at 20°C and 66/10/18/6 at 32°C as compared with the membrane 55%CER6/25%Ch/15%PA/5%ChS (SC_PA) at 32°C (Kiselev et al. 2005)

Composition	Repeat distance at 57% RH (Å)	z_{PH} (Å)[a]	Thickness of hydrophilic region (Å)	Thickness of hydrophobic region (Å)[b]
55/20/15/10	45.67 ± 0.02	22.75 ± 0.01	7.8 ± 0.2	30 ± 0.2
66/10/18/6	45.6 ± 0.2	22.68 ± 0.01	8.0 ± 0.2	29.4 ± 0.2
SC_PA	45.63 ± 0.04	22.82 ± 0.01	7.2 ± 0.2	31.2 ± 0.1

[a] z_{PH} is the position of the Gaussian function corresponding to the polar head groups

[b] Thickness of hydrophobic region = $2z_{HH}$

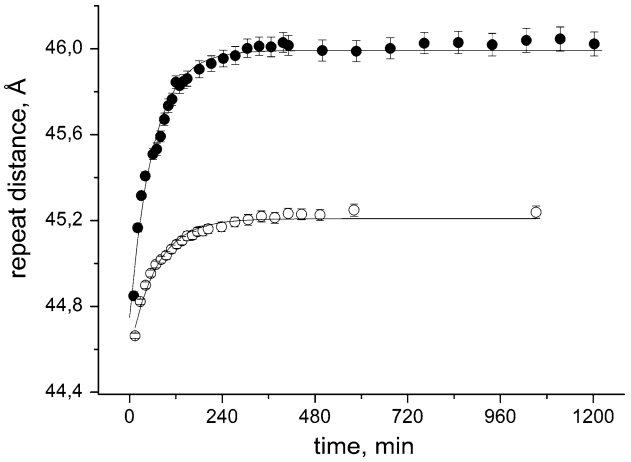

Fig. 5 Hydration of the CER6/Ch/FFA/ChS membranes with the compositions 55/20/15/10 (*circles*) and 55/30/15/0 (*open circles*) measured in D_2O excess at 20°C

(Fig. 7) is split into two phases with repeat distances of 45.79 ± 0.07 and 44.11 ± 0.03 Å.

Discussion

The aim of the present work is to characterize SC model membranes with near-native free fatty acid mixture by neutron diffraction. Previously, for the first time, the internal structure at 60% humidity and the hydration process of oriented model SC membranes composed of CER6, cholesterol, palmitic acid, and cholesterol sulfate (55/25/15/5 w/w) were characterized using neutron diffraction (Kiselev et al. 2005). Analysis of the neutron scattering length density distribution (profile) $\rho(z)$ allowed us to describe the internal structure of a multibilayer membrane. The low hydration of the intermembrane space at 60% humidity as well as at water excess (about 1 Å for a fully hydrated membrane) was found as a marked distinction of this SC system from phospholipid membranes. In the present study we examined the system CER6/Ch/FFA/ChS (55/20/15/10 and 66/10/18/6 w/w) at the same experimental conditions to compare its structure with that of the SC_PA membrane (reference system).

The diffraction pattern of the CER6/Ch/FFA/ChS membrane at the weight ratio 55/20/15/10 shows a nearly one-phase system with periodicity of 45.7 Å. At temperature of 32°C diffraction spectrum reveals the second minor structure phase with repeat distance of 44.0 Å. The CER6/Ch/FFA/ChS mixture at the weight ratio 60/20/15/5 is also a quasihomogeneous system with the same repeat distance of the main phase of 45.7 Å. The existence of some structurally different phases with long-range ordering in a sample becomes apparent in the presence of Bragg peaks from these phases in a diffraction pattern. Here we identify the presence of more than one phase with close repeat distance in the sample by the asymmetry of the higher-order peaks, the most resolved in the reciprocal-space. The system whose diffraction pattern contains *completely unresolved* diffraction peaks from different structural phases we shall

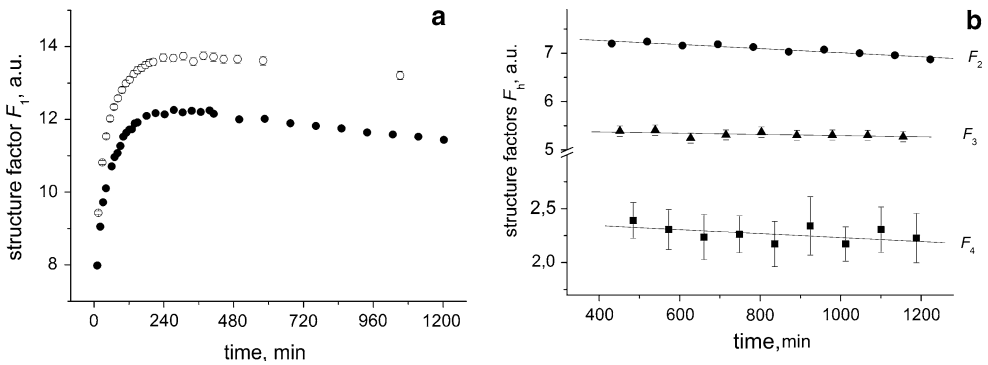

Fig. 6 **a** Time dependence of the first structure factor of the CER6/Ch/FFA/ChS membranes with compositions 55/20/15/10 (*circles*) and 55/30/15/0 (*open circles*) measured at 20°C during swelling in D_2O. **b** Time dependence of the structure factors of the CER6/Ch/FFA/ChS membrane with composition 55/20/15/10

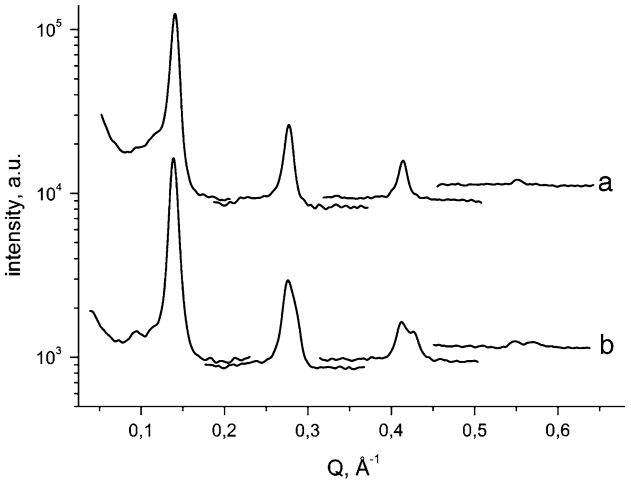

Fig. 7 Neutron diffraction spectra from the fully hydrated CER6/Ch/FFA/ChS membranes with compositions *a* 55/20/15/10 and *b* 55/30/15/0 measured at 20°C

call "near-one-phase system" or "quasihomogeneous system", and define hereinafter the absolute values of structural factors of such system from the general integrated intensity of peaks. Recovered as a Fourier transformation of the thus-defined experimental structural factors, the scattering length density distribution contains information on the *phase-average* internal structure of bilayers.

In the CER6/Ch/FFA/ChS system with the lipid composition 66/10/18/6, a separate minor phase with periodicity of ~53 Å is present. Most likely, this phase is formed by pure longer-chain C22:0 and C24:0 fatty acids. In the work of Ruettinger and coworkers the study of CER6/Ch/FA/ChS systems (55/25/15/5 w/w) based on individual fatty acids revealed that longer-chain free fatty acids tend to form a new separate so-called fatty-acid-rich phase, and the periodicity of the main phase decreases with an increase in the free fatty acid chain length (Ruettinger et al. 2008). It is notable that the presence of a mixture of six free fatty acids with different chain length in the membrane with the same percentage of FFA (15%) inhibits separation of individual free fatty acids from the multilamellar structure. This result agrees with the finding of Jager and coworkers that the presence of free fatty acids with varying acyl chain length facilitates the incorporation of lipids into the lamellar phase in the lipid mixtures (Jager et al. 2003).

Visual comparison of the neutron scattering length density distribution of the CER6/Ch/FFA/ChS systems with that of the SC_PA membrane shows the similarity of internal structure of these systems, whose main feature is a small intermembrane space. To compare the structure of these systems quantitatively, the Fourier profiles were fitted by a model function formerly used for a reference system (Kiselev et al. 2005). The greater thickness of the hydrophilic region of the FFA-based systems (~8 Å) than of the reference system (7.2 Å) is explained by replacement of a part of cholesterol by cholesterol sulfate in the membrane composition. The thicknesses of the hydrophobic region amount to 30 and 29.4 Å for the CER6/Ch/FFA/ChS membranes with compositions 55/20/15/10 and 66/10/18/6, respectively, which is slightly smaller in comparison with that of the SC_PA membrane (31.2 Å). This narrowing of hydrophobic core can be a result of an increase in the tilt angle of the hydrocarbon chains with respect to the membrane plane. The same effect was observed by Ruettinger et al. (2008) in membranes with individual fatty acids. Partially interdigitated chains of free fatty acids create some free space. FFA fill this space by titling their chains in order to minimize free volume inside the membrane.

Considerably slower membrane swelling at water excess as compared with phospholipid membranes was a typical feature of the SC_PA membrane. In the present investigation the repeat distance of the FFA membrane increases exponentially with a characteristic time of 61 ± 2 min, which is one and a half times faster than for the SC_PA membrane. This increase in membrane swelling rate is likely caused by a less dense bilayer arising from interdigitation of the longer-chain fatty acids. The mobility of the lipid molecules in this system is higher than in a more compact membrane with only short-chain palmitic acid and may promote the flip-flop transition of CER6 molecules, which becomes visible as a decrease in the characteristic time of membrane swelling.

The decrease in the first structure factor F_1 after 2 h swelling can be explained by supposing that any change in the internal membrane structure occurs due to hydration. In the work of Kiselev and co-workers a drastic decrease in the value of the first-order diffraction peak of the SC_PA membrane was observed after 1 h hydration in water excess. To explain this jumping of intensity, the flip-flop transition of CER6 molecules was suggested (Kiselev et al. 2005). Under membrane hydration the CER6 molecule changes its FE conformation for an energetically favorable one-side conformation (OS conformation), and as a result the adjacent bilayers move apart and the membrane repeat distance increases by approximately 1 Å compared with the partially hydrated state of the system. Similar structural alterations of fully hydrated porcine SC were observed by neutron diffraction (Charalambopoulou et al. 2002). After 15 h of hydration in D_2O the period of lamellar structure of SC tissue increases from 57 Å at 100% RH to 70 Å. Interestingly, under prolonged hydration (up to 8 days) the repeat distance remained unchanged, whereas the first-order peak disappeared, but the second weak peak did not change. This effect of hydration on native SC can also be explained by the flip-flop transition of ceramide molecules from FE conformation to OS conformation. In the present work the flip-flop transition of CER6 molecules could

cause a linear decrease in F_1. On the other hand, Fig. 6 presents a monotonic decrease in all measured structure factors, which could also be caused by sample dissolution in the water.

Two effects of ChS on the fully hydrated SC model membranes have been observed. First, the replacement of ChS by Ch does not change the hydration rate, while the increase in the cholesterol/cholesterol sulfate ratio from 2/1 up to 3/0 leads to twofold lower swelling of the ChS-free membrane: $\Delta d = 0.63 \pm 0.02$ Å versus 1.24 ± 0.02 Å for the ChS-containing membrane. Such effect of ChS on hydration of phospholipid membranes has been earlier observed using microscopy, X-ray diffraction, nuclear magnetic resonance (NMR) techniques, and molecular dynamics simulation (Faure et al. 1996; Smondyrev and Berkowitz 2000). The greater swelling of ChS-containing membrane is not surprising and is most likely caused by the ability of a sulfate group of ChS to form many more hydrogen bonds with water as compared with the hydroxyl group of Ch. Second, ChS stabilizes the membrane. The membrane without ChS splits into two phases. This phase separation could arise from a decrease in lipid mobility in the absence of ChS. The negatively charged sulfate group of ChS increases the molecular area per lipid and thus reduces the lipid packing density and increases the lipid mobility in the bilayer, thus promoting the miscibility of the lipids.

Summing up the presented results, one can conclude that the structure of the partially hydrated model SC systems based on the mixture of six free fatty acids in a temperature range of 20–32°C is close to that of the system based on palmitic acid with characteristic small interbilayer space. The variation of the main component ratio does not lead to any significant change of membrane structure parameters and denotes a very stable membrane nanostructure reinforced by CER6 molecules. The free fatty acid composition accelerates the membrane swelling as compared with the SC membrane based on short-chain palmitic acid at the same level of hydration of both PA- and FFA-containing membranes. The replacement of cholesterol by cholesterol sulfate in the membrane composition increases the membrane swelling, inhibits the phase separation, and thereby leads to a more homogeneous lipid system. The presented data support the hypothesis that cholesterol sulfate promotes intercellular cohesion of SC by increasing the stability of intercellular membranes.

References

Bouwstra JA, Gooris GS, van der Spek JA, Bras W (1991) Structural investigations of human stratum corneum by small-angle X-ray scattering. J Invest Dermatol 97:1005–1012

Bouwstra JA, Gooris GS, Cheng K, Weerheim A, Bras W, Ponec M (1996) Phase behavior of isolated skin lipids. J Lipid Res 37:999–1011

Bouwstra JA, Gooris GS, Dubbelaar FER, Weerheim AM, Ijzerman AP, Ponec M (1998) Role of ceramide 1 in the molecular organization of the stratum corneum lipids. J Lipid Res 39:186–196

Bouwstra JA, Gooris GS, Dubbelaar FER, Ponec M (1999) Cholesterol sulfate and calcium affect stratum corneum lipid organization over a wide temperature range. J Lipid Res 40:2303–2312

Bouwstra JA, Dubbelaar FER, Gooris GS, Ponec M (2000) The lipid organisation in the skin barrier. Acta Derm Venereol Suppl 208:23–30

Breathnach AS, Goodman T, Stolinski C, Gross M (1973) Freeze fracture replication of cells of stratum corneum of human epidermis. J Anat 114:65–81

Bueldt G, Gally HU, Seelig A, Seelig J, Zaccai G (1978) Neutron diffraction studies on selectively deuterated phospholipid bilayers. Nature 271:182–184

Charalambopoulou GC, Steriotis TA, Mitropoulos AC, Stefanopoulos KL, Kanellopoulos NK, Ioffe A (1998) Investigation of water sorption on porcine stratum corneum by very small angle neutron scattering. J Invest Dermatol 110:988–990

Charalambopoulou GC, Steriotis TA, Hauss T, Stefanopoulos KL, Stubos AK (2002) A neutron diffraction study of the effect of hydration on stratum corneum structure. Appl Phys A Suppl 74:1245–1247

Elias PM (1983) Epidermal lipids, barrier function, and desquamation. J Invest Dermatol 80:44–49

Elias PM, Williams ML, Holleran WM, Jiang YJ, Schmuth M (2008) Pathogenesis of permeability barrier abnormalities in the ichthyoses: inherited disorders of lipid metabolism. J Lipid Res 49:697–714

Faure C, Tranchant JF, Dufourc EJ (1996) Comparative effects of cholesterol and cholesterol sulfate on hydration and ordering of DMPC membranes. Biophys J 70:1380–1390

Franks NP, Lieb WR (1979) The structure of lipid bilayers and the effects of general anaesthetics. J Mol Biol 133:469–500

Garson JC, Doucet J, Leveque JL, Tsoucaris G (1991) Oriented structure in human stratum corneum revealed by X-ray diffraction. J Invest Dermatol 96:43–49

Jager MW, Gooris GS, Dolbnya IP, Bras W, Ponec M, Bouwstra JA (2003) The phase behaviour of skin lipid mixtures based on synthetic ceramides. Chem Phys Lipids 124:123–134

Jager MW, Gooris GS, Dolbnya IP, Bras W, Ponec M, Bouwstra JA (2004) Novel lipid mixtures based on synthetic ceramides reproduce the unique stratum corneum lipid organization. J Lipid Res 45:923–932

Kessner D, Kiselev M, Dante S, Hauss T, Lersch P, Wartewig S, Neubert RHH (2008) Arrangement of ceramide [EOS] in a stratum corneum lipid model matrix: new aspects revealed by neutron diffraction studies. Eur Biophys J 37:989–999

Kiselev MA (2007) Conformation of ceramide 6 molecules and chainflip transitions in the lipid matrix of the outermost layer of mammalian skin, the stratum corneum. Crystallogr Rep 54(3):549–553

Kiselev MA, Ryabova NY, Balagurov AM, Dante S, Hauss T, Zbytovska J, Wartewig S, Neubert RH (2005) New insights into the structure and hydration of a stratum corneum lipid model membrane by neutron diffraction. Eur Biophys J 34:1030–1040

Lampe MA, Burlingame AL, Whitney J, Williams ML, Brown BE, Rittman E, Elias PM (1983) Human stratum corneum lipids: characterization and regional variations. J Lipid Res 24:120–130

Madison KC, Schwartzendruber DC, Wertz PW, Downing DT (1987) Presence of intact intercellular lamellae in the upper layers of the stratum corneum. J Invest Dermatol 88:714–718

McIntosh T (2003) Organization of skin stratum corneum extracellular lamellae: diffraction evidence for asymmetric distribution of cholesterol. Biophys J 85:1675–1681

McIntosh TJ, Stewart ME, Downing DT (1996) X-ray diffraction analysis of isolated skin lipids: reconstitution of intercellular lipid domains. Biochemistry 35:3649–3653

Norlén L, Emilson A, Forslind B (1997) Stratum corneum swelling. Biophysical and computer assisted quantitative assessments. Arch Dermatol Res 289:506–513

Rand RP, Luzzati V (1968) X-ray diffraction study in water of lipids extracted from human erythrocytes: the position of cholesterol in the lipid lamellae. Biophys J 8:125–137

Robson KJ, Stewart ME, Michelsen S, Lazo ND, Downing DT (1994) 6-Hydroxy-4-sphingenine in human epidermal ceramides. J Lipid Res 35:2060–2068

Ruettinger A, Kiselev MA, Hauss TH, Dante S, Balagurov AM, Neubert RHH (2008) Fatty acid interdigitation in stratum corneum model membranes: a neutron diffraction study. Eur Biophys J 37:759–771

Schoenborn BP (1976) Neutron scattering for the analysis of membranes. Biochim Biophys Acta 457:41–55

Smondyrev AM, Berkowitz ML (2000) Molecular dynamics simulation of dipalmitoylphosphatidylcholine membrane with cholesterol sulfate. Biophys J 78:1672–1680

Strott CHA, Higashi Y (2003) Cholesterol sulfate in human physiology: what's it all about? J Lipid Res 44:1268–1278

White SH, Mirejovsky D, King GI (1988) Structure of lamellar lipid domains and corneocyte envelopes of marine stratum-corneum-a x-ray diffraction study. Biochemistry 27:3725–3732

Williams ML, Elias PM (1981) Stratum corneum lipids in disorders of cornification. I. Increased cholesterol sulfate content of stratum corneum in recessive X-linked ichthyosis. J Clin Invest 68:1404–1410

Worcester DL, Franks NP (1976) Structural analysis of hydrated egg lecithin and cholesterol bilayers. II. Neutron diffraction. J Mol Biol 100:359–378

Zbytovska J, Kiselev MA, Funari SS, Garamus VM, Wartewig S, Palat K, Neubert R (2008) Influence of cholesterol on the structure of stratum corneum lipid model membrane. Colloids Surf A Physicochem Eng Asp 328:90–99

Zettersten E, Man MQ, Sato J, Denda M, Farrell A, Ghadially R, Williams ML, Feingold KR, Elias PM (1998) Recessive X-linked ichthyosis: role of cholesterol-sulfate accumulation in the barrier abnormality. J Invest Dermatol 111:784–790